R&D NOTES

Reactor Analysis with Diffusion-Limited, Concentration-Dependent Deactivation

A. S. Krishna
Chevron Research & Technology Co.
Richmond, CA 94802

J. R. Kittrell
KSE Inc.
Amherst, MA 01004

The influence of mass transfer resistances on concentration-independent decay was examined by Krishnaswamy and Kittrell (1981a,b, 1982). Poisoning of catalytic-active sites, however, is often caused by an impurity in the feed stream or by reactants and products themselves. For porous catalysts undergoing such concentration-dependent deactivation, the impact of intraparticle diffusional resistances was studied by Masamune and Smith (1966). The results of their numerical effectiveness factor for reactant-induced (parallel) deactivation were shown to be useful for predicting conversion-time behavior in fixed-bed reactors. However, the complexity of their numerical solution prohibits easy interpretation of deactivation data. Tai and Greenfield (1981) used an approximate analytical solution for the time-dependent effectiveness factor to model parallel deactivation in a fixed-bed reactor. They analyzed pore diffusion-limited experimental data on the deactivation of immobilized catalase during hydrogen peroxide decomposition and obtained a value for the intrinsic deactivation rate constant which was three to five times larger than the apparent deactivation rate constant associated with various particle sizes.

For the case of a first-order reaction and first-order, concentration-independent deactivation, Krishnaswamy and Kittrell (1981a) showed that deactivation data can be analyzed in terms of rate equations with associated rate constants. Linearized ln ln $(1/1 - x)$ vs. time plots were obtained, and slopes were related to the apparent rate of decay in order to obtain an intrinsic deactivation rate constant. When severe pore diffusion limitations were present, the apparent deactivation rate constant was shown to be one-half the intrinsic value. In this paper, the possibility of extending this approach to analyze concentration-dependent decay is investigated. The parallel deactivation model used for this purpose is similar to that of Masamune and Smith (1966).

Single Particle Equations

The mass conservation equations for an isothermal, spherical particle with first-order reaction and deactivation, in dimensionless form, are:

$$\frac{\partial^2 y}{\partial R^2} + \frac{2}{R}\frac{\partial y}{\partial R} - \phi^2 y a = 0 \tag{1}$$

$$\frac{\partial a}{\partial t} + \Psi^2 y a = 0 \tag{2}$$

and

$$\begin{aligned} a &= 1.0 \quad \bar{t} = 0;\ 1 \geq \mathrm{R} \geq 0 \\ y &= \bar{y} \quad R = 1.0;\ \bar{t} \geq 0 \\ \frac{\partial y}{\partial R} &= 0 \quad R = 0;\ \bar{t} \geq 0 \end{aligned} \tag{3}$$

Equations 1, 2 and 3 were solved using an implicit finite difference scheme. In dimensionless form, the pellet effectiveness factor, defined as the ratio of the overall rate for the particle to the rate at surface conditions, with unit catalyst activity, is:

$$\eta_t = \frac{1}{3h^2}\frac{\partial y}{\partial R}\bigg|_{R=1.0}\frac{1}{\bar{y}} \tag{4}$$

where $h = (\phi/3)$, the Thiele modulus.

Correspondence concerning this paper should be addressed to A. S. Krishna, formerly known as S. Krishnaswamy, at P.O. Box 1627, Richmond, CA 94802.

Plots of the catalytic effectiveness as a function of dimensionless time θ (where $\theta = \Psi^2 \cdot \bar{t}$), with h as parameter, are similar to those of Masamune and Smith (1966) for parallel deactivation.

Reactor Analysis

The time-dependent catalytic effectiveness thus derived can be substituted in mass balances for flow reactors in order to predict the effect of internal diffusion limitations on conversion-time behavior.

Stirred-tank reactor

The mass balance for a stirred-tank reactor configuration is:

$$\frac{x}{1-x} = \eta_t \tau \qquad (5)$$

where η_t is given by Eq. 4.

Figure 1 shows plots of ln η_t vs. θ, with h as parameter. When diffusion limitations are absent, Eq. 2 can be solved directly (by setting $y = 1$) to obtain:

$$\eta_t = a = \exp(-\theta) \qquad (6)$$

Consequently, the plot for $h = 0$ is linear, with a slope of unity. It is apparent from Figure 1 that the ln η_t vs. θ plots {and hence plots of ln $[x/(1-x)]$ vs. θ} are approximately linear for values of h greater than zero. The slope of the lines decreases continuously with increasing values of h. When diffusion limitations are severe, the slope approaches zero, suggesting that the catalyst ceases to deactivate under such extreme conditions.

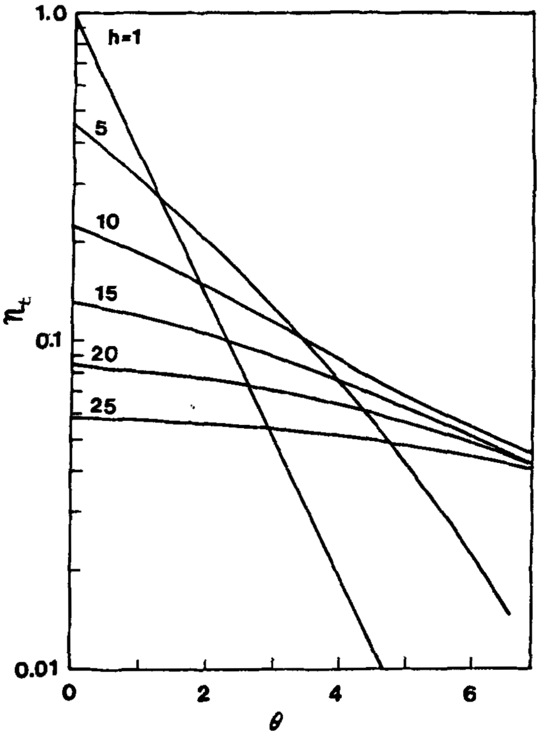

Figure 1. Effectiveness factor vs. dimensionless time.

Fixed-bed reactor

Assuming pseudosteady state and plug flow, the mass balance for a fixed-bed reactor can be written as (Masamune and Smith, 1966):

$$\frac{\partial \bar{y}}{\partial \bar{z}} + \bar{y}\eta_t = 0 \qquad (7)$$

Masamune and Smith solved Eq. 7 (with $\bar{y} = 1.0$ at $\bar{z} = 0$) numerically, using an approximate form of the catalytic effectiveness, given by the shell model. In the present investigation, the exact numerical solution for the effectiveness factor was used in conjunction with Eq. 7 to predict conversion-time behavior.

Results and Discussion

Figure 2 shows plots of η_t as a function of dimensionless bed length $\bar{z}$, with θ as parameter, for three values of the Thiele modulus. At zero time, the catalyst activity is unity and the mass balances are identical to those for a first-order, nondeactivating system. The catalytic effectiveness is given by the conventional

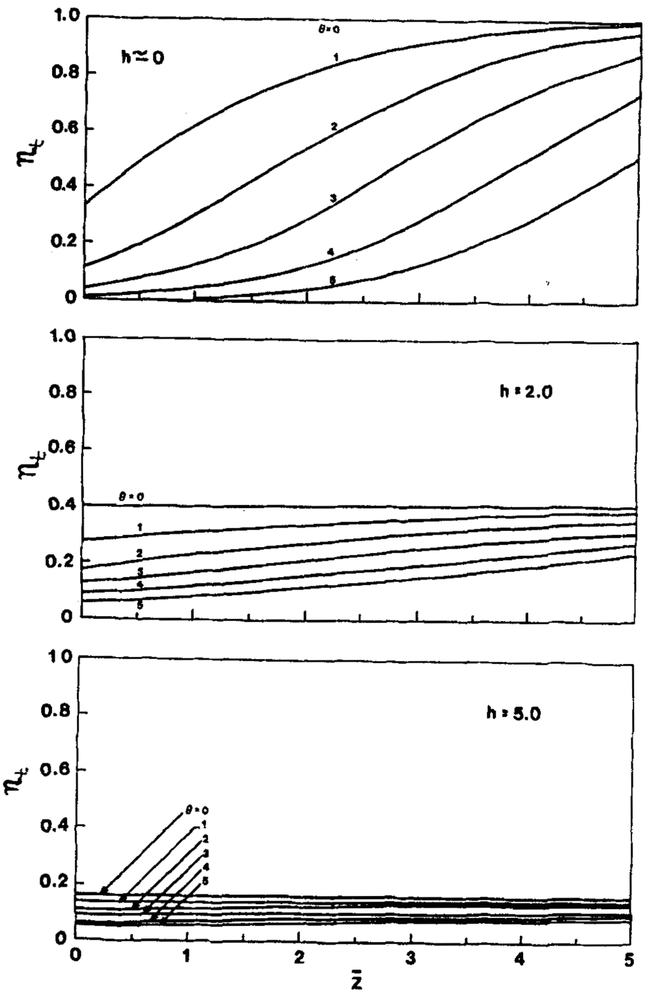

Figure 2. Effectiveness factor profiles in catalyst bed.

isothermal effectiveness factor relationship (Smith, 1970). For first-order kinetics, the effectiveness factor is independent of reactant concentration and is therefore invariant with bed lengths as shown by Figure 2. For dimensionless time values greater than zero, the catalyst activity drops below unity and the primary reaction kinetics are no longer first order in reactant concentration. As the rate of the main reaction decreases with increasing bed length, diffusion limitations, by contrast, become less significant. Consequently, the effectiveness factor increases gradually from its initial value, with distance down the reactor bed. The plots of Figure 2 show that, as the diffusion limitations are increased, the catalytic effectiveness decreases and the curves of η_t vs. $\bar{z}$ become flatter. Approximate solutions utilizing this constant value of η_t may be useful.

When $h = 0$, Eq. 6 applies, and an analytical solution exists for Eq. 7. The resulting conversion-time relationship is given by Krishnaswamy and Kittrell (1978).

$$\ln\left(\frac{x}{1-x}\right) = \ln k' - \theta \tag{8}$$

where

$$k' = [\exp(k\tau) - 1]$$

and

$$\theta = (k_d \cdot C_{Ao} \cdot t)$$

Hence, experimental data for diffusion-free systems, when plotted as $\ln[x/(1-x)]$ vs. t will be linear for parallel deactivation, with the slope being a measure of the intrinsic deactivation rate constant times the feed reactant concentration. [The slope of the $\ln[x/(1-x)]$ vs. θ plot will of course be unity.]

From Figure 3, it is seen that such plots are approximately linear even when diffusion limitations are present. The slope of the lines decreases with increasing diffusion limitations and approaches zero asymptotically, similar to those of Figure 1 for the single particle.

Hence, for both stirred-tank and fixed-bed reactor configurations, there is reason to expect that the analysis of Krishnaswamy and Kittrell (1981a) for concentration-independent decay can be extended to apply for parallel deactivation. It may then be possible to use Eq. 8 to describe parallel deactivation, even under the presence of internal diffusion limitations, with θ now being given by:

$$\theta = k_{dp} \cdot C_{Ao} \cdot t$$

and

$$k_{dp} = k_d \cdot \eta_d \tag{9}$$

The deactivation effectiveness factor η_d would vary from unity for no diffusion to values approaching zero under conditions of extreme diffusion limitations.

The analysis of concentration-dependent deactivation data is, however, expected to be complicated by several factors. For example, since the rate of decay is a function of reactant concentration, the plots of Figure 3 will depend on the conversion level of operation. Under conditions of extreme diffusion limitations, only the outer core of the particle is accessible to the reactant. The bulk of the catalyst is shielded from the deactivation-causing reactant, and hence changes in reactant concentration have little or no impact on decay rate. However, for low to intermediate values of h, it is expected that the impact of differing conversion levels will be more significant; for these cases, the analysis will be burdened by the fact that η_d will be a function of the reactant concentration. Furthermore, Krishnaswamy and Kittrell (1981a,b) have shown that, when resistances to external mass transfer also exist, the lower limit on η_d, for concentration-independent decay, can approach zero. Hence, techniques have to be developed that will help distinguish between the effects of concentration independent and dependent decay as well as the presence of internal and external transport resistances.

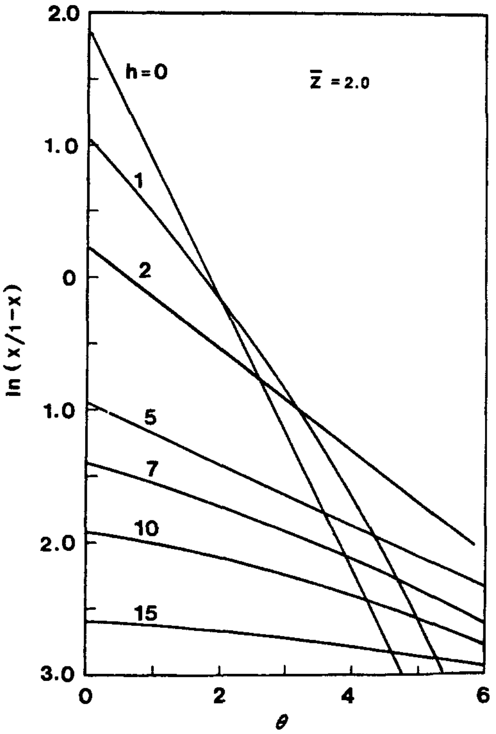

Figure 3. Conversion function vs. dimensionless time.

Analysis of Experimental Data

The decomposition of hydrogen peroxide by immobilized catalase serves as an excellent system for testing independent and parallel deactivation models. Under conditions of very low substrate concentration and high temperature, the decay rate would be independent of substrate. Experimental data, under these conditions, were obtained by Krishnaswamy and Kittrell (1982). Parallel decay models would apply for experimental data taken at high substrate and low temperature levels, such as those of Altomare et al. (1974).

Conversion-time data of both Altomare et al. and Krishnaswamy and Kittrell were plotted as $\ln[x/(1-x)]$ vs. time, as shown in Figures 4 and 5, respectively. The data of Altomare et

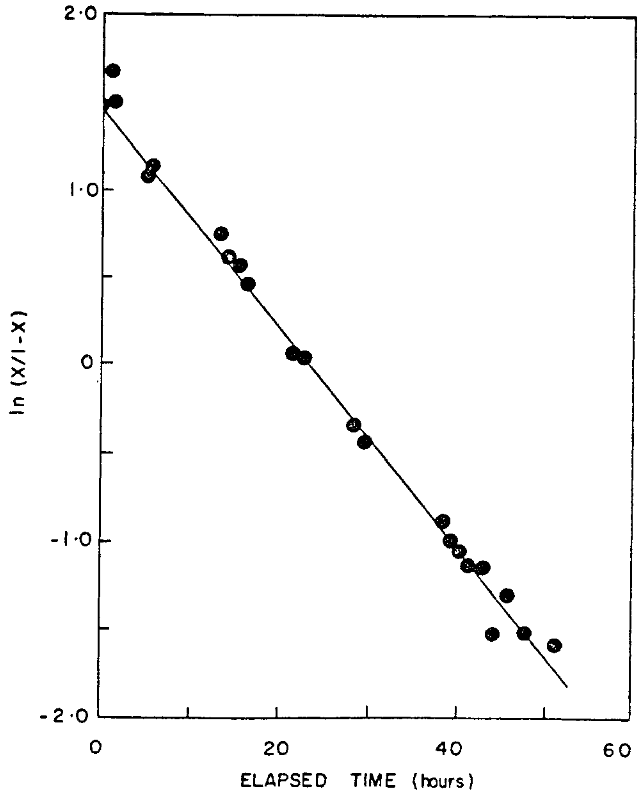

Figure 4. Conversion function vs. dimensionless time.
Data of Altomare et al. (1974)

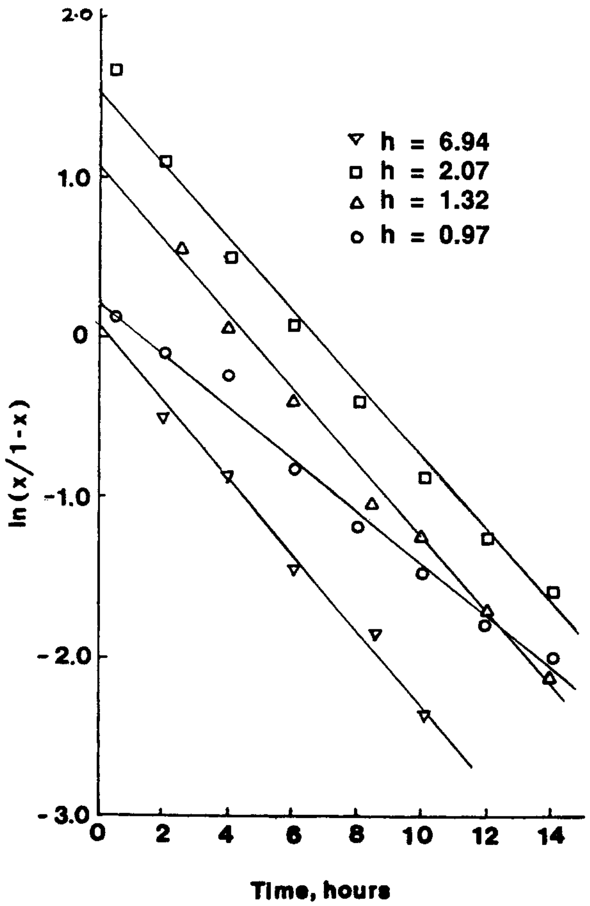

Figure 5. Conversion function vs. dimensionless time.
Data of Krishnaswamy and Kittrell (1982)

al. were taken under conditions of severe internal diffusion limitations. It is encouraging to note that the plot of Figure 4, within experimental error, is linear. This lends support to the suggestion that it should be possible to develop deactivation models that predict such linear behavior and relate slopes to intrinsic deactivation parameters.

Since concentration-independent decay can be considered as a limiting case of parallel deactivation (i.e., for very low reactant concentrations), intuitively we would expect the data of Krishnaswamy and Kittrell to also plot linearly as $\ln\,[x/(1-x)]$ vs. t, at least for extremes of diffusion limitations. This is indeed the case, as shown by the plots of Figure 5.

Concluding Remarks

Concentration-independent deactivation data are found to plot linearly as $\ln\ln\,[1/(1-x)]$ vs. t (Krishnaswamy and Kittrell, 1982), as well as $\ln\,[x/(1-x)]$ vs. t (this paper) for extremes of diffusion limitations, since a concentration-independent deactivation model is equivalent to a parallel deactivation model for very low substrate levels. Clearly, the converse is not true, and the data of Altomare et al. taken under condition of high substrate concentrations will not be expected to plot linearly as $\ln\ln\,[1/(1-x)]$ vs. t. In fact, such plots were found to exhibit large deviations from linearity. On the basis of the analyses of experimental and theoretical conversion-time behavior in flow reactors presented in this paper, there is reason to believe that simple techniques can be developed to interpret concentration-dependent deactivation data under the presence of diffusion limitations.

Notation

a = fractional catalyst activity
C_{Ao} = reactant concentration at the outer surface of particle, gmol/cm^3
D_A = effective diffusivity of reactant inside particle, cm^2/s
F_{Ao} = reactant feed rate, gmol/s
h = Thiele modulus ($= \phi/3$)
k = Rate constant for primary reaction, s^{-1}
k_d = rate constant for deactivation, cm^3/s · gmol
k_{dp} = pseudodeactivation rate constant ($= k_d \cdot \eta_d$)
r_s = radius of spherical particle, cm
R = dimensionless radial position ($= r/r_s$)
t = process time, s
$\bar{t}$ = dimensionless time ($= t \cdot D_A/r_s^2$)
u = superficial velocity, cm/s
W = weight of catalyst, g
x = fractional conversion
y = dimensionless concentration inside particle ($= C_A/C_{Ao}$)
$\bar{y}$ = dimensionless interparticle concentration
z = length, cm
$\bar{z}$ = dimensionless length ($= k \cdot \rho_B \cdot z/\rho u$)

Greek letters

η_t = dimensionless effectiveness factor, Eq. 4
η_d = dimensionless deactivation effectiveness factor
θ = dimensionless time ($= \Psi^2\,\bar{t}$)
ρ = particle density, g/cm^3
ρ_B = bulk density, g/cm^3
τ = dimensionless space time $\{= [(W \cdot C_{Ao})/F_{Ao}](k/\rho)\}$
ϕ = dimensionless group $[= r_s\sqrt{(k/D_A)}]$
Ψ = dimensionless group $[= r_s\sqrt{(k_d \cdot C_{Ao}/D_A)}]$

Literature Cited

Altomare, R. E., P. F. Greenfield, and J. R. Kittrell, "Inactivation of Immobilized Fungal Catalase," *Biotechnol. Bioeng.*, **16**, 1675 (1974).

Krishnaswamy, S., and J. R. Kittrell, "Diffusional Influences on Deactivation Rates," *AIChE J.*, **27**, 125 (1981a).

———, "The Effect of External Diffusion on Deactivation Rates," *AIChE J.*, **27**, 125 (1981b).

———, "Diffusional Influences on Deactivation Rates: Experimental Verification," *AIChE J.*, **28**, 273 (1982).

Krishnaswamy, S., and J. R. Kittrell, "Deactivation Disquised Kinetics," *I&E Proc. Des. Dev.*, **27**, 200 (1978).

Levenspiel, O., *Chemical Reaction Engineering*, 2nd ed. Wiley, New York (1972).

Masamune, S., and J. M. Smith, "Performances of Fouled Catalyst Pellets," *AIChE J.*, **12**, 384 (1966).

Smith, J. M., *Chemical Engineering Kinetics*, 2nd ed. McGraw-Hill, New York (1970).

Tai, N. M., and P. F. Greenfield, "Determination of the Inherent Deactivation Characteristics for the Parallel Poisoning of Immobilized Catalase," *Biotechnol. Bioeng.*, **23**, 805 (1981).

Manuscript received Jan. 8, 1990, and version received Feb. 9, 1990.